Hindawi
International Journal of Energy Research
Volume 2023, Article ID 7787947, 14 pages
https://doi.org/10.1155/2023/7787947

Research Article

High-Dimensional Model Representation-Based Surrogate Model for Optimization and Prediction of Biomass Gasification Process

Yousaf Ayub,[1] **Jianzhao Zhou**,[1] **Jingzheng Ren**,[1] **Tao Shi**,[1] **Weifeng Shen**,[2] **and Chang He**[3]

[1]*Department of Industrial and Systems Engineering, The Hong Kong Polytechnic University, Hong Kong SAR, China*
[2]*Department of Chemistry and Chemical Engineering, Chongqing University, Chongqing 400044, China*
[3]*School of Materials Science and Engineering, Guangdong Engineering Centre for Petrochemical Energy Conservation, Sun Yat-sen University, Guangzhou 510275, China*

Correspondence should be addressed to Jingzheng Ren; renjingzheng123321@163.com

Received 14 October 2022; Revised 10 January 2023; Accepted 11 January 2023; Published 6 February 2023

Academic Editor: Kathiravan Srinivasan

Biomass gasification process has been predicted and optimized based on process temperature, pressure, and gasifying agent ratios by integrating Aspen Plus simulation with the high-dimensional model representation (HDMR) method. Results show that temperature and biomass to air ratio (BMR) have significant effects on gasification process. HDMR models demonstrated high performance in predicting H_2, net heat (NH), higher heating value (HHV), and lower heating value (LHV) with coefficients of determination 0.96, 0.97, 0.99, and 0.99, respectively. HDMR-based single-objective optimization has maximum outputs for H_2, HHV, and LHV (0.369 of mole fractions, 340 kJ/mol, and 305 kJ/mol, respectively) but NH would be negative at these conditions, which indicates that process is not energy-efficient. The optimal solution was determined by the multiobjective which produced 0.24 mole fraction of H_2, 158.17 kJ/mol of HHV, 142.48 kJ/mol of LHV, and 442.37 kJ/s NH at 765°C, 0.59 BMR, and 1 bar. Therefore, these parameters can provide an optimal solution for increasing gasification yield, keeping process energy-efficient.

1. Introduction

Biomass waste utilization is one of the potential methods that can help to minimize GHG emissions while satisfying energy demands through syngas production. Amount of hydrogen in the syngas is one of the primary indicators of quality syngas. H_2 is also one of the environment friendly energy vectors which has a wide range of application in energy and agriculture sectors but it is not naturally available. Therefore, it needs to be produced through different technologies which are debatable among researchers in terms of sustainability issues. However, some renewable energy technologies like solar and wind power have been applied to produce more sustainable hydrogen [1]. Gasification process can be used to synthesize the H_2 from biomass waste which is also a renewable energy source. Thermal and biological methods can be utilized to transform the biomass waste into different types of energy or value-added compounds. Pyrolysis and gasification are the two primary thermal conversion processes, whilst anaerobic and aerobic digestion are the biological processes that can be applied to valorize biomass waste [2]. Researchers have extensively studied these processes, and each process has its own technoeconomic, energy, exergy, and environmental benefits and drawbacks [2]. Therefore, H_2 energy vector can be produced through biomass waste gasification process which could be sustainable in terms of economic, environment, and energy efficiency.

Poultry litter biomass gasification process is the scope of this study, which is one of the feasible and cost-effective thermochemical process for biomass valorization. The final product of the biomass gasification process is syngas, which

is a mixture of CO, CO_2, H_2, and CH_4. The quality of syngas is determined by the biomass type, particle size, and process parameters such as reaction temperature and gasifying agent (air, steam, and O_2) [3]. Process operating conditions including temperature, pressure, and gasifying agents have significant effect on output. Therefore, strive to get the optimum process operating conditions is important but still challenging [4]. Gasification process temperature and gasifying agent also have significant effects on the syngas quality because it promotes the decomposition of biomass into lower molecular weight gases such as CO, CO_2, H_2, and CH_4 [5]. According to research findings, increasing gasifying agents (air, O_2, steam, CO_2, etc.) can contribute to higher energy efficiency of the output by increasing H_2 content in syngas [5, 6]. Similarly, higher temperature range in 800-900°C promotes more H_2 production in gasification process while low temperature produces char and CH_4 [2, 7]. Thus, the biomass feedstock types, its particles size, and process parameters such as temperature and gasifying agent can influence syngas yield in the gasification process.

Prediction and optimization of the gasification process can be done using process simulation and mathematical modeling. Thermodynamic equilibrium and kinetic models are the two primary aspects for biomass gasification modeling and simulation. In thermodynamic modeling, Gibbs free energy minimization has been applied to obtain the thermodynamic property of chemical processes while kinetic modeling is more accurate compared with thermodynamic models to predict the gasification process [8, 9]. Application of kinetic modeling in simulation model development has more stringent requirements in contrast to thermodynamics, but high-performance computing simulation programs have made it amenable to simulate it [10]. Aspen Plus® is one of the process-based simulation software which has been widely applied for chemical process simulation based on thermodynamics and kinetic modeling [11]. Process modeling is feasible by using simulation software, but model input parameters need to be changed for yield prediction, which are limited to the availability of the respective model, simulation software, and significance expertise that are also required. Hence, the process yield prediction model with high accuracy is required which can predict the output without considering the aforementioned constraints.

There are various techniques adopted by researchers for biomass waste valorization process optimization and prediction. Vascellari et al. [12] proposed a technique for validation and application of the kinetic parameters to predict and optimize the process output. Dang et al. [13] applied the kinetic model for biomass gasification process prediction and optimization using Aspen Plus software. Another method was proposed by Hashimoto et al. [14], and it is related to the detailed data extraction from the biomass valorization experimental or simulation studies for database development, but interpolation of the intermediate values is not possible in such technique. Xing et al. [15] developed an artificial neural network (ANN) model to predict valorization process output based on process parameters. Kargbo et al. [16] applied ANN for the prediction of syngas from two-stage gasification process, and coefficient of determinant (R^2) for all element of syngas was greater than 0.99 with the exception of CO_2 and N_2 which have R^2 in the range of 0.74-0.82. Ascher et al. [17] also applied ANN for the prediction of gasification process output based on input parameter syngas quality, feedstock, and reactor type, and the R^2 for this model was 0.9310. In addition to the prediction accuracy, complex chemical reactions were involved in gasification process which needs to be represented by high dimensional models. This leads to high computational cost and also difficult in optimization by application of traditional mathematical techniques [18]. Machine learning and neural network models are preferable option for predicting output based on some algorithms, but these models use backbox approach that ignores variable interactions, while kinetic modeling has its own set of limitations in terms of complexity and expertise. Therefore, a better prediction and optimization approach is required for gasification process which has better computational power, processing flexibility, and efficient in terms of gasification prediction and optimization.

The high-dimensional model representation (HDMR) method is a tool for recording the input-output relationships of high-dimensional systems. It is a mathematically proven and efficient processing model because it shifts from exponential scaling to polynomic complexity, which significantly reduces computational effort [19]. In comparison to "black box" models such as ANN, the HDMR model can be easily used to describe the relationships between variables due to the explicit expression. Furthermore, as an objective function, there is a flexibility in algorithms due to its simple mathematical structure, which gives it advantages in algorithm selectivity for process optimization. Rabitz and Brownbridge et al. have developed this which has been widely used to deal with complex situations in chemical processes such as predictive model construction, global uncertain analysis, and economic assessment [19, 20]. Pan et al. [18] has applied the high dimensional model representation (HDMR) for chemical process optimization in ecoindustrial parks. Azadi et al. [21] applied HDMR in the global sensitivity analysis of lower heating value (LHV), cold gas efficiency (CGE), and gas yield from algae biomass. Singh and Tirkey [22] had applied response surface methodology (RSM) for multiobjective optimization of Syzygium cumini biomass gasification performance. H_2, CGE, and HHV optimum values were reported to have 0.1 (mole fraction), 25.23%, and 3.96 MJ/kg, respectively. Xie et al. [23] obtained the best operating solutions in a propane dehydrogenation process for high efficiency by application of HDMR-based surrogate models. Han et al. 2021 concluded comparatively weak dependence of HDMR on training data size and a strong ability to assess the sensitivity of output to input variable for predicting dual-fuel ignition delay time [24]. Therefore, these HDMR-based surrogate models have been categorized into data-driven which uses the data generated from the complex simulation models or experiment for prediction purpose [25]. Considering the advantages of HDMR over neural network and database approach, the HDMR-based data-driven model is being developed for gasification output prediction using methodology defined in Section 2.3. A

dataset has been generated using a validated Aspen Plus simulation model given in Section 2.2, and then this dataset is used to establish a surrogate model while reduces the complexity compared with the physical model. Finally, this HDMR data-driven model is applied for process optimization by using the methodology presented in Section 2.4. Gasification process prediction and optimization with net energy constraint and the multiobjective optimization have been carried out considering the following objective:

(i) Prediction and multiobjective optimization of hydrogen yield (H_2), HHV, and LHV in poultry litter gasification process by application of HDMR

2. Methodology

Gasification process simulation has been developed with the help of literature-based experimental data. This model has been validated against the experimental studies by application of different types of biomasses, and then, the HDMR prediction model has been developed based on this validated version of simulation. Detail of this research methodology is given in Sections 2.1-2.3.

2.1. Process Flow. Process flow diagram of the research method has been given in Figure 1. Gasification process simulation data was collected from the different biomass gasification process-related studies [26–28]. Reaction kinetics and mass flow balance were considered while developing the gasification process simulation model. This simulation model had been experimentally validated by comparing it with four different types of biomasses. For process validation, root mean square error (RMSE) against each biomass type was calculated. Design of experiments (DOE) given in Table 1 was used to obtain the necessary results for prediction model development and optimization. For DOE, gasification process input parameters such as temperature, pressure, and gasifying agent (air) have been altered to produce different syngas outputs as different studies proposed these process parameters have significant effect on the process output. Therefore, range of these process parameters have been taken from literature which have been analyzed by one factor change at a time using DOE [5–7, 28]. Mole fractions of hydrogen, lower heating value, higher heating value, and net heat are the key performance indicators of this simulation process. While net heat value signifies the net process energy efficiency, therefore, net heat value should be greater than zero which can be calculated by using Eq. (3). For NH, HEATSRM block has been used in the simulation (Figure 2) which calculates the total net heat of all reactors. The HDMR-based prediction model has been developed based on the design of experiment data. Validity of this model has been confirmed by using coefficient of determination (R^2), mean square error (MSE), mean relative error (MRE), and mean absolute error (MAE). Finally, the HDMR results have been concluded in Section 4.

2.2. Process Simulation Model. The process simulation model has been developed by using Aspen Plus. Four different types of biomass waste including poultry litter, soft wood, mix wood, and sewage sludge saw dust have been analyzed for simulation model validity which is given in Section 2.2.2. Biomass waste is a nonconventional (NC) material; therefore, proximate and ultimate analyses of the biomass have been used as a feed taken from the experimental study which have been obtained through feedstock analysis using IKA C5000 calorimeter, Flash 2000 CHNS analyzer, and NETZSCH STA 449 F3 Jupiter Thermogravimeter [28]. This proximate and ultimate analyses (Table 2) have been used as nonconventional feedstock in the simulation model. For HDMR-based prediction, poultry litter biomass yield results have been collected by multiple simulation runs as given in Section 2.2.2.

In this simulation model, the Peng Robinson Equation of States (PR) method is applied due to its better results when the output is in the form of low molecular weight gases such as CO, CO_2, H_2, and CH_4 [11]. Model has been developed based on Gibbs free energy minimization given in these studies [26, 27]. The total Gibbs energy of the reaction can be calculated using the consolidated Eqs. ((1)) and ((2)) obtained through studies [26, 27].

$$\text{Total Gibbs Energy of the reaction } (G_T) = \sum_{i=1}^{N} n_i \Delta G_{f,i}^{o} + \sum_{i=1}^{N} n_i RT \ln \frac{n_i}{n_{\text{tot}}}, \quad (1)$$

where n_i represents the total concentration of mole, $\Delta G_{f,i}^{o}$ is the standardized form of Gibbs free energy formations, and R and T represent general gas constant and temperature, respectively.

By application of the Lagrange multiplier method, Gibbs free energy can be minimized as given in Eq. (2). In Aspen Plus software, the process simulation model has followed these equations for chemical process modeling.

Using Lagrange multiplier, Gibbs energy can be minimized as given in the below equation:

$$\frac{\delta L}{\delta n_i} = \Delta G_{f,i}^{o} + n_i RT \ln \frac{n_i}{n_{\text{tot}}} + \sum_{j=1}^{k} a_{ij} \mathcal{E}_j, \quad (2)$$

where $\mathcal{E}_j$ is the Lagrange multiplier, L is the Lagrange function, and a_{ij} represents the j-th element in the i-th mole of the compound equations for chemical process modeling.

Gasification parameters have been taken from the literature [5–7, 28]. Temperature ranges for gasification have been specified by the researcher from 400 to 1000°C in different studies [5–7, 28]. Therefore, temperature range for this research study has been selected from 400 to 1000°C with an interval of 100°C. Similarly, the effect of pressure variation on the gasification yield has also been analyzed. The correlating effect of four different pressure levels including 1, 2, 3, and 4 bars has been analyzed to investigate its effects on H_2, HHV, LHV, and NH. Air is used as gasifying agent in the process; hence, different ratios of biomass to air (BMR) have been evaluated. Seven different levels of BMR including

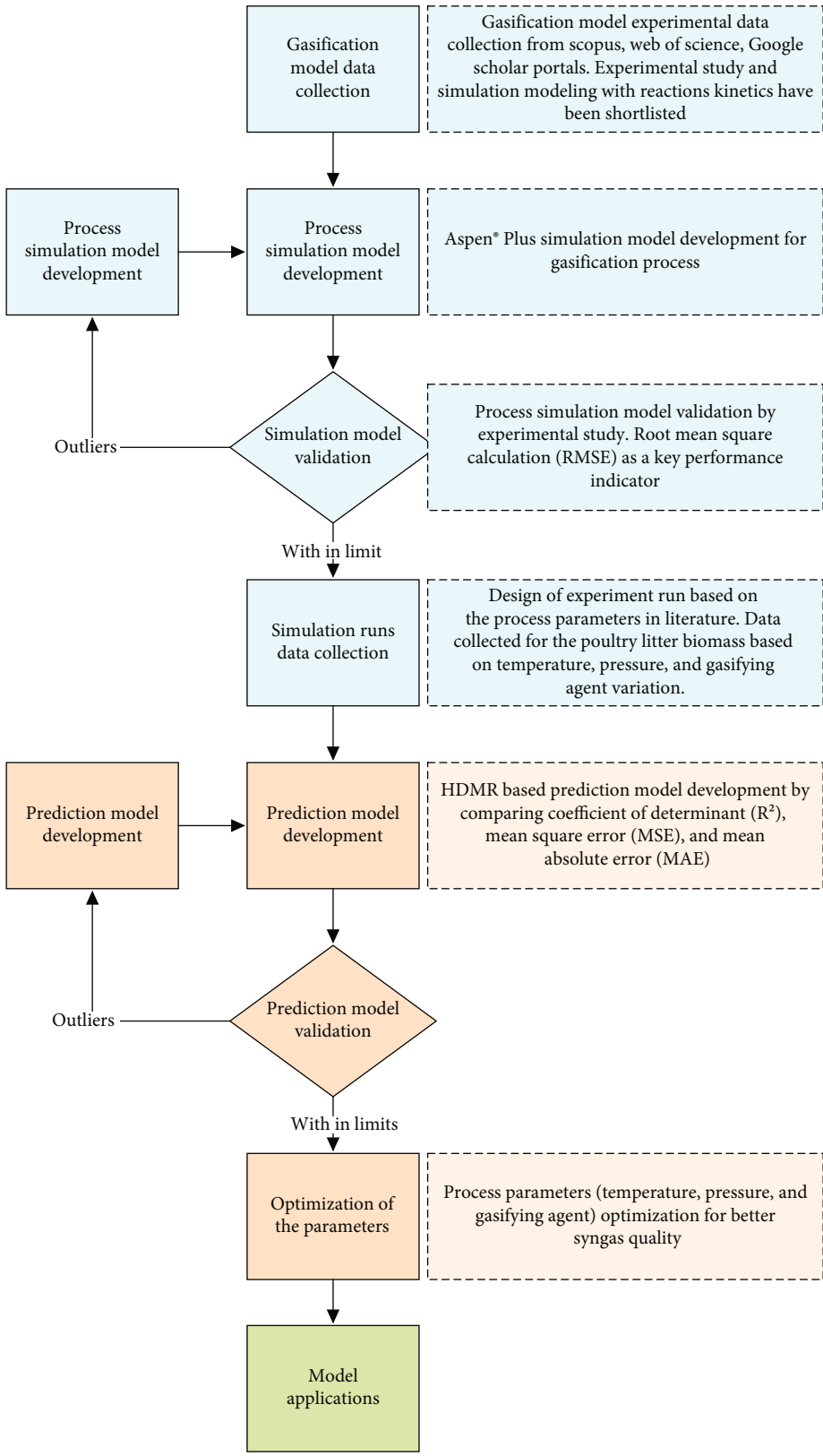

Figure 1: Research methodology.

Table 1: Design of experiment model [5–7, 28].

Temperature °C (T)	Pressure bar (P)	Biomass to air ratio (BMR)	Model runs (196)
400	1	0.25	$T_{ij} \times P_{ij} \times \mathrm{BMR}_i = 28$
500	2	0.33	$T_{ij} \times P_{ij} \times \mathrm{BMR}_i = 28$
600	3	0.50	$T_{ij} \times P_{ij} \times \mathrm{BMR}_i = 28$
700	4	0.75	$T_{ij} \times P_{ij} \times \mathrm{BMR}_i = 28$
800	—	1.00	$T_{ij} \times P_{ij} \times \mathrm{BMR}_i = 28$
900	—	1.33	$T_{ij} \times P_{ij} \times \mathrm{BMR}_i = 28$
1000	—	2.00	$T_{ij} \times P_{ij} \times \mathrm{BMR}_i = 28$

where T_{ij} is the respective individual value of temperature, P_{ij} is the pressure value, and BMR_i is the respective individual air ratio.

0.25, 0.33, 0.5, 0.75, 1, 1.33, and 2.0 have been applied to examine the results on the gasification output.

Process simulation has been developed on Aspen Plus by selecting the Peng Robinson Equation of State (PR) method, and the feed rate is 1000 kg/hr. For process simulation, it is assumed that the model is in steady state, and the isothermal condition with no heat or material loss in the reactors was used [11]. Biomass enthalpy of formation, HCOALGEN, and DCOALIGT property models have been selected [29]. Enthalpy, specific heat capacity, and density are determined based on ultimate and proximate analyses of the biomass. C, CO, CO_2, H_2, CH_4, H_2O, and N_2 components have been selected for the model. Finally, ash is considered as a nonconventional solid which is nonreactive. Gasification process has been divided into different subprocesses, starting from the dry biomass intake in the PYRO reactor. It is RStoic reactor in which fraction conversions of the biomass have been set at specified temperature with respect to the chemical reactions' stoichiometry [30]. In PYRO block, fractional conversions of poultry litter biomass have been taken as an input. These fractions have been given in Table 3 which are calculated based on elemental stoichiometry ratios. Temperature and pressure of the reactor block vary from 400 to 1000°C and 1-4 bar, respectively, as per Table 1. Products produced from PYRO reactor have been separated by SEP1 into solid residue and gases. For further syngas recovery, residue is further processed in the DECOMP block to produce gases (CO, CO_2, H_2, and CH_4) at 400-1000°C and 1-4 bar which combines with air and gas coming from SEP1 in the mixer block. Combustion of this gas mixture has been simulated by using the COMBUST (RPlug) block with specified reaction kinetics which have been taken from the literature [30, 31]. This is the main block which converts biomass waste into syngas in the presence of oxygen at 400-1000°C, 1-4 bar, and 0.25-2 BMR. Quality of produced syngas in COMBUST block is not good. Therefore, further reforming of the COMBUST block syngas has been done to make process more realistic and closer to experimental results. Finally, reduction of the outlet COMBUS stream has been done in REDUCT (RPlug) block at 400-1000°C and 1-4 bar to get syngas which also includes reaction kinetics taken from the literature [31].

$$N^h = \sum_{i=1}^{n} H_b, \tag{3}$$

where N^h is the net heat stream and H_b is the heat stream of the respective block (PYRO, DECOMP, COMBUST, and REDUCT).

This syngas has been validated with experimental results, which is given in Section 2.2.1. The net heat stream has been calculated, which is one of the key indicators to check the process feasibility in terms of energy. Equation (3) has been used to calculate the net heat stream. The process simulation model has been applied for this calculation. Heat streams of all blocks including PYRO, DECOMP, COMSTRM, and REDSTRM have been connected into a mixer block (HEATSRM) as given in Figure 2. This block calculates the net heat stream (NHSTR, Figure 2) of the simulation model. Higher net stream depicts more energy efficiency of the process.

2.2.1. Validation of Simulation Model. The gasification process simulation model has been validated by experimental results [28]. Four different types of biomasses including poultry litter, softwood pellets, mix wood pellets, and sewage sludge saw dust have been used to validate the process simulation model. Mole fractions of H_2, CO, CO_2, and CH_4 produced in the simulation model have been compared with the experiment results. Comparison of the mole fractions in experimental and that determined by the simulation models has been given in Figure 3. Furthermore, the root means square errors (RMSE) of these comparative results have also been calculated to obtain the overall results error. RMSE has been calculated by using Eq. (4) [32]. Poultry litter (PL) experimental (Exp.) and simulation (Sim.) values are close to each other, similarly for the mix wood (MC), soft wood (SW), and sewage sludge saw dust (SS) values that are bit closer which reflect the more accuracy of the developed model.

$$\mathrm{RMSE} = \sqrt{\sum_{i=1}^{n} \frac{(S_i - A_i)^2}{n}}, \tag{4}$$

where RMSE represents the root mean square error, A_i represents the experimental value of the element, S_i represents the simulation model value, i is the respective element (the i-th element), and n represents the total number of elements in comparison.

The RMSE between the poultry litter simulation data and the experimental results is 1.5% which shows that the results of the simulation model are close to the experimental results. The RMSEs with respect to mix wood waste and soft wood are 4.2% and 4.8%, respectively, while it is 3.3% for sewage sludge saw dust. All RMSEs in the validation are less than 5% especially with respect to poultry litter, and it is 1.5% which is a sign of higher accuracy in the simulation model.

2.2.2. Data Collection from Validated Simulation Model. Validated process simulation of gasification has been employed

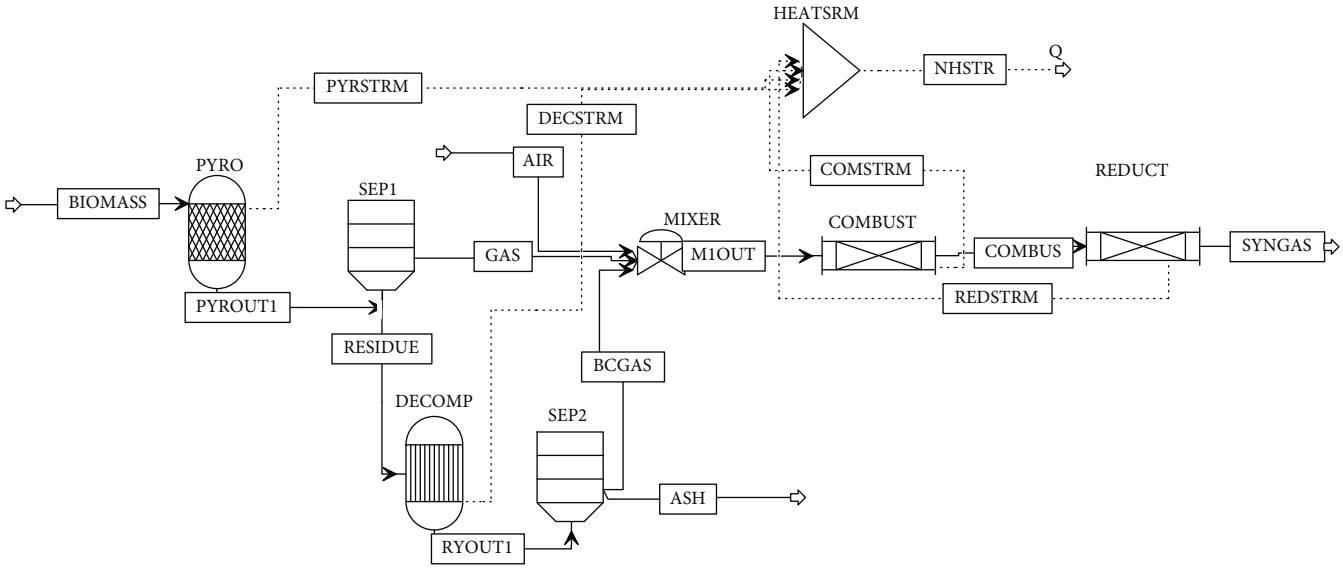

Figure 2: Aspen Plus gasification process simulation model.

Table 2: Proximate and ultimate analyses of biomass waste [28].

		Poultry litter	Softwood chips	Mix wood chips	Sewage-saw dust sludge
Ultimate analysis	Moisture	7.6	5.2	10.6	4.4
	Carbon	43.98	49.2	48.77	41.08
	Hydrogen	5.16	6.2	5.85	5.51
	Oxygen	31.98	44.06	44.52	26.9
	Nitrogen	4.63	0.08	0.05	3.77
	Sulphur	0.75	0.06	0.01	0.94
Proximate analysis	Volatile matter	63.6	79.2	75.8	59.5
	Fix carbon	15.3	15.2	12.8	14.3
	Ash	13.5	0.4	0.8	21.8
	HHV (MJ/kg)	16.8	19.0	17.3	17.8

Table 3: PYRO fractional conversion of poultry litter (PL) biomass.

Reactants	*R*-coefficient	Products	*P*-coefficient	Fraction conversion of BM
PL	-1	CH_4	0.06233	0.06453
PL	-1	H_2	0.49606	0.00601
PL	-1	CO	0.03570	0.33908
PL	-1	CO_2	0.02272	0.29918
PL	-1	H_2O	0.05551	0.00047
PL	-1	BIOCHAR	1	0.29073

for data collection which is further used for the development of the HDMR model. For this purpose, design of experiment has been developed with three independent variables of process parameters. Temperature, pressure, and gasifying agent (air) ratio have been used as the inputs because different studies have revealed that gasification process output is dependent on these process parameters irrespective of biomass types [5–7, 28]. Multilevels of these input parameters have been selected as mentioned in Section 2.2. Seven levels of temperature from 400 to 1000°C with increment of 100°C, four levels of pressure 1-4 bars, and seven levels of BMR 0.25, 0.33, 0.5, 0.75, 1, 1.33, and 2.0 have been selected in the simulation model for data collection. Multiple runs of the validated simulation model with poultry litter biomass have been carried out because simulation results of poultry litter gasification were better than others. Mole fractions of H_2, CO_2, and CO along with the higher heating value (HHV), lower heating values (LHV), and net heat have been collected. The data collected from the validated simulation runs have been used to develop the HDMR model for multi-objective optimization.

2.3. High-Dimensional Model Representation (HDMR) Model. The HDMR model has been developed for prediction and optimization of gasification process [19]. In HDMR, the output variable is expressed as a sum of functions that depends on subsets of the input variables schematically given in Figure 4 model while it is expressed mathematically

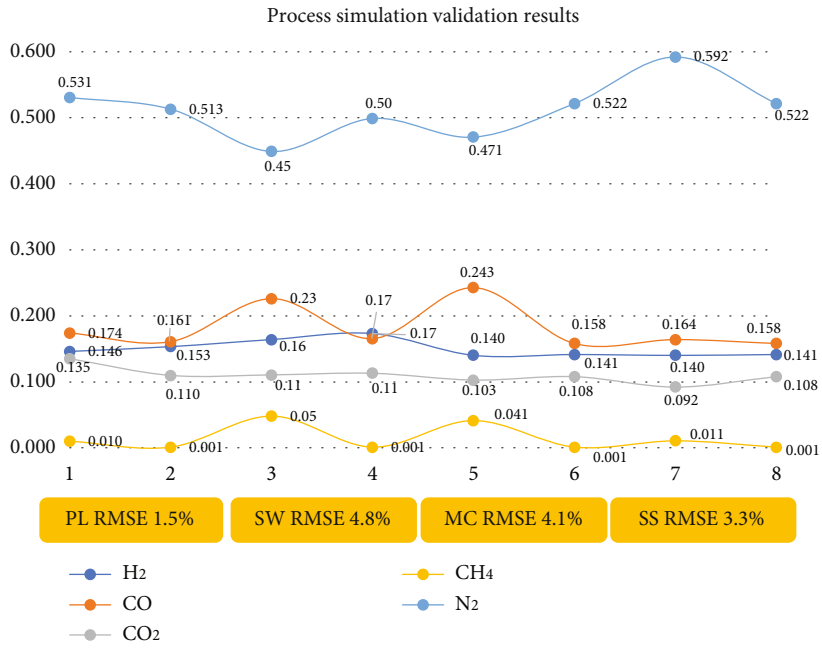

Figure 3: Comparisons of experimental results and simulation data [28].

in Eq. (5) [33]. Temperature, pressure, and gasifying agent (air) ratio have been set as inputs for HDMR while H_2, CO_2, HHV, LHV, and NH values are the outputs of the model.

$$y = f_0 + \sum_{i=1}^{N} f_i(x_i) + \sum_{i=1}^{N}\sum_{j=i+1}^{N} f_{ij}(x_i x_j) + \cdots + f_{12\cdots N}(x_1 x_2 \cdots x_N), \tag{5}$$

where f_0 denotes the zeroth order effect which is a constant, N is the number of input parameters, i and j index the input parameters, $f_i(x_i)$ represents the effect of the i-th input variable to the output y, and $f_{ij}(x_i x_j)$, $f_{12\cdots N}(x_1 x_2 \cdots x_N)$, indicates the correlated effect contributed by two input variables (x_i, x_j) and all the input variables $(x_i, x_j \cdots x_N)$ to output, respectively.

Due to the nonlinear features of gasification process, higher-order polynomial terms are required to obtain accurate results. As given in Eq. (6), a better model expression was adopted to generate surrogate models for describing biomass gasification process [18]. Equation (6) can be seen as a truncated approximation of Eq. (5) [18].

$$y = C + \sum_{i=1}^{N}\sum_{k=1}^{K} A_{i,k} \times x_i^k + \sum_{i=1}^{N}\sum_{j=i+1}^{N}\sum_{k=1}^{K}\sum_{n=1}^{K} B_{i,j,k,n} \times x_i^k \times x_j^n, \tag{6}$$

where C is a constant term, $A_{i,k}$ and $B_{i,j,k,n}$ are the first- and second-order coefficients, K is the highest degree of input variables, subscripts i and j denote the input parameters, and y is the function value.

For better training efficiency, K has been parameterized (as hyperparameters) in this study, and then, the training of the HDMR model has been converted into polynomial regression problem. The coefficients including C, $A_{i,k}$, and $B_{i,j,k,n}$ were obtained by least squares. For evaluating the performance of HDMR surrogate models, coefficient of determination (R^2), mean square error (MSE), mean absolute error (MAE), and mean relative error (MRE) in test set are calculated by Eqs. (7)–(12) [34, 35]. Data has been normalized before using the algorithms for effective analysis and processing.

$$\mathrm{SS}_{\mathrm{res}} = \sum_{i}^{n} \left(y_i^{\mathrm{pre}} - y_i\right)^2, \tag{7}$$

$$\mathrm{SS}_{\mathrm{tot}} = \sum_{i}^{n} \left(y_i^{\mathrm{pre}} - y_i^{\mathrm{mean}}\right)^2, \tag{8}$$

$$R^2 = 1 - \frac{\mathrm{SS}_{\mathrm{res}}}{\mathrm{SS}_{\mathrm{tot}}}, \tag{9}$$

$$\mathrm{MAE} = \sum_{i}^{n} \frac{\left|y_i^{\mathrm{pre}} - y_i\right|}{n}, \tag{10}$$

$$\mathrm{MSE} = \frac{\mathrm{SS}_{\mathrm{res}}}{n}, \tag{11}$$

$$\mathrm{MRE} = \sum_{i}^{n} \frac{\left|y_i^{\mathrm{pre}} - y_i\right|}{y_i \times n} \times 100\%, \tag{12}$$

where y_i^{pre} is the i -th predicted output value, y_i is the i -th output value in dataset, n is the amount of data in dataset, and $\mathrm{SS}_{\mathrm{res}}$ represents explained sum of squares while $\mathrm{SS}_{\mathrm{tot}}$ represents total sum of squares.

The HDMR data-driven models for different outputs have named as H_2 model (for predicting the mole fraction

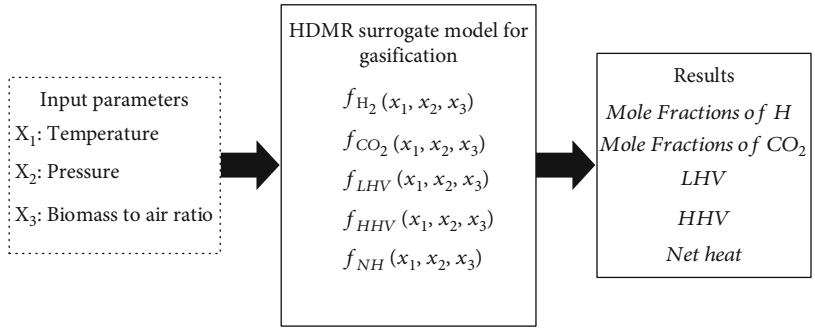

Figure 4: HDMR surrogate model illustration.

of hydrogen in the products), similarly for CO_2, HHV, LHV, and NH models. The training process obtains the parameters A, B, and C with minimum error between model results and the training data which has been programmed in MATLAB. For this, data generated from the Aspen Plus model is divided into 75% training set and 25% testing set. Training data is employed to determine the best hyperparameter K based on the 10-fold method and based on the K results [18, 19], and then, the model can be generated. Finally, 25% testing data is used to test the model for assessing the predictability of the established model by calculating the MSE, MAE, and MRE.

2.4. Gasification Process Optimization. Multiobjective optimization has done by application of nonlinear programing (NLP) based the problem model which is given in the following equation [36].

$$\min \quad f(x), \tag{13}$$

$$s.t. \quad h_t(x) = 0, \tag{14}$$

$$g_m(x) \le 0, \tag{15}$$

where $f : R^n \longrightarrow R, h : R^n \longrightarrow R^t$, and $g : R^n \longrightarrow R^m$ are smooth functions. For solving easier, the nonlinear program (Eq. (13–15)) could be replaced by a sequence of barrier subproblems of the form

$$\begin{aligned} \min \; & Z(x,s) = f(x) - \mu \sum_{i=1}^{m} \ln s_i \\ & s.t. h_t(x) = 0, \\ & g_m(x) + s = 0 \end{aligned} \tag{16}$$

where $\mu > 0$ is the barrier parameter and the slack variable s is assumed to be positive. By decreasing values of μ, the sequence of solutions to Eq. (16) should normally converge to a stationary point of the original nonlinear program Eq. (13–15).

According to MATLAB function "fmincon" used in this study, the process can be described as follows. The Lagrangian function associated with Eq. (16) is defined by [37]

$$L(x, s, \lambda_h, \lambda_g) = Z(x, s) + \lambda_h^T h(x) + \lambda_g^T (g(x) + s), \tag{17}$$

where λ_h and λ_g are the Lagrange multipliers.

The Karush-Kuhn-Tucker (KKT) conditions have been solved to

$$\begin{aligned} \frac{\partial Z}{\partial x} &= 0, \\ \lambda_i g_i(x) &= 0, \\ \lambda_i &\ge 0, \\ \lambda_i h_i(x) &= 0, \\ \lambda_i &\ge 0. \end{aligned} \tag{18}$$

The Hessian H of $L(x, s, \lambda_h, \lambda_g)$ is

$$H = \nabla^2 f(x) + \sum_i \lambda_i \nabla^2 g_i(x) + \sum_j \lambda_j \nabla^2 h_j(x). \tag{19}$$

The Hessian (H) transforms into a matrix form and which can be solved by any quasi-Newton methods. If the computation fails, conjugate gradient step is used to solve KKT conditions. It has been determined to minimize a quadratic approximation to the problem $Z(x, s)$ keeping the solution in the trust region. After determining the search direction, the appropriate step size needs to be found. The interior point method (IPM) uses a decrease in merit function approach until the final stop tolerance is achieved, where the resulted function is the combination of the objective function with the absolute value of the constraint violation times ν, as presented in Eq. (20) [38] if it is a better step or not.

$$Z(x, s) + \nu \| h(x), g(x) + s \|, \tag{20}$$

where parameter ν may increase with the iterations for feasibility of solution (20) [38], if it is a better step or not.

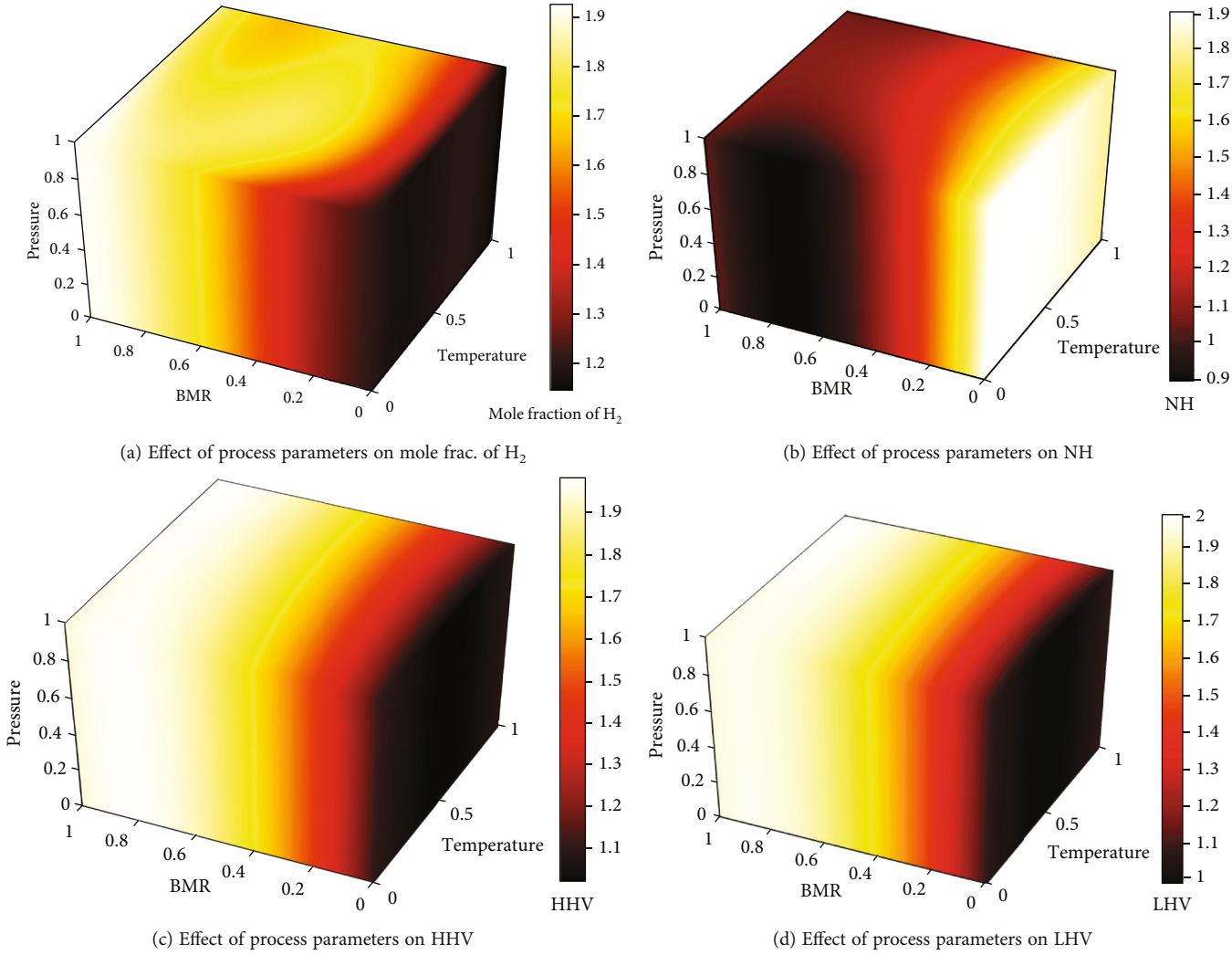

(a) Effect of process parameters on mole frac. of H_2

(b) Effect of process parameters on NH

(c) Effect of process parameters on HHV

(d) Effect of process parameters on LHV

Figure 5: Effect of gasification process parameters.

3. Results and Discussions

Result analysis and discussion for the simulation model and HDMR surrogate model have been carried out, and descriptions of these results are given in Sections 3.1 and 3.2.

3.1. Effect of Simulation Process Parameters. The effect of process parameters including temperature, pressure, and gasifying agent (BMR) on mole fractions of H_2, NH, HHV, and LHV has been illustrated in Figure 5. According to Figure 5(a), increasing BMR improves the mole fractions of hydrogen in syngas, and pressure has no significant effect on the mole fractions of hydrogen, while temperature also shows substantial effects on H_2 yield in syngas. Mole fractions of the H_2 have been increased with increasing temperature around 700°C. These findings are also consistent with the previously published work [39, 40].

Process net heat (NH), an indication of energy efficiency, has an inverse relationship with BMR, as shown in Figure 5(b). NH increases as BMR drops in the process, and NH has direct impact due to temperature. Temperature has a considerable effect on NH; temperatures above 800°C promote less NH, and pressure has little effect on NH. Increasing pressure shows somehow positive change in NH. The HHV and LHV show nearly identical patterns and trends with BMR, pressure, and temperature. HHV and LHV are directly connected with BMR; increasing BMR has a significant positive influence on them, while pressure has no effect.

Increasing BMR improves syngas HHV and LHV, whereas temperature has a correlation with HHV and LHV, with lower temperature having better HHV and LHV, as illustrated in Figures 5(c) and 5(d), respectively. According to Figure 5, the gasifying agent (BMR) is the primary factor contributing to the mole fractions of H_2, HHV, LHV, and NH at 700°C, whereas pressure has no significant effect on these process outputs. Therefore, BMR is the most significant process parameter affecting the output of mole fractions of H_2, NH, LHV, and HHV while temperature is also a contributing factor which affects the mole fractions of H_2.

3.2. HDMR Surrogate Model Analysis. As a hyperparameter, the maximum degree of input variables K

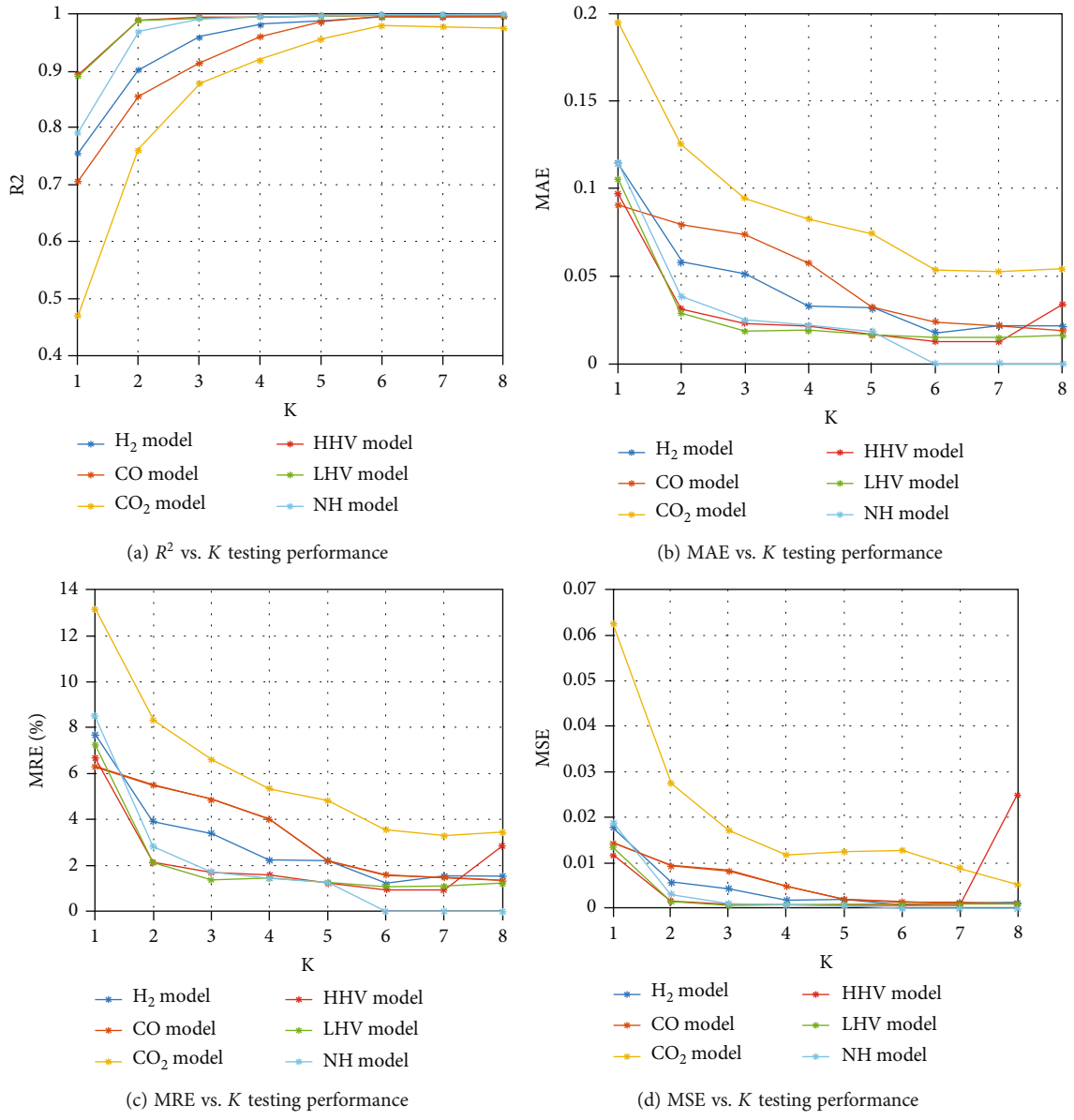

(a) R^2 vs. K testing performance

(b) MAE vs. K testing performance

(c) MRE vs. K testing performance

(d) MSE vs. K testing performance

Figure 6: HDMR model testing performance with respect to K.

represents model complexity. The accuracy of the HDMR surrogate model changes with K, which has been investigated to establish the optimal parameter K in the models for future application. A higher K value in the model can result in model overfitting. Therefore, to prevent overfitting, K value keeps low for HHV, LHV, NH, H_2, CO, and CO_2, as given in Tables S1-S6. Furthermore, 10-fold crossvalidation methods were used in this process to avoid model overfitting. The training performances (R^2) have been improved significantly with the increase of K as presented in Figure 6(a). According to this, the training of models could get better R^2 when K is being increased from 1 to 8 but increasing K value also increases the risk of overfitting. Therefore, lower K value is better for the prediction model development. Specifically, R^2 for H_2, HHV, LHV, and NH models is greater than 0.95 when $K = 4$ which means that the model can perform better prediction for these output variables. As per Figure 6, more complex model (higher K) has good fitness (R^2) in the training process. Therefore, the model's output performance in terms of mean absolute error (MAE), mean square error (MSE), and percentage mean relative error (%MRE) was also evaluated using the training set. The test set's increasing K values in MAE (Figure 6(b)), MRE (Figure 6(c)), and MSE (Figure 6(d)) have been investigated. The results of Figure 6(b) show that the H_2, HHV, LHV, and NH models produced higher accuracies with MAE less than 0.05 at $K = 5$. MRE of these parameters is less than 3% at $K = 5$ in Figure 6(c). Mean square error (MSE) of H_2, HHV, LHV, and NH is less than 0.01 at $K = 2$ which represents the better model performance in terms of MSE prediction for these

parameters. Therefore, based on Figure 6 data, $K = 3$ has been set for optimal prediction of H_2, HHV, LHV, and NH with the lesser risk of overfitting.

Dataset based on different simulation runs has been divided into test set and training set with 0.25 and 0.75 ratios, respectively, to get the optimum prediction results. Then, models for different outputs were obtained (the coefficients are shown in supplementary Tables S1-S6). The training performance of these models is given in Figure 6. The R^2 of these models lied between 0.90 and 0.99, which means that all models are well trained for better prediction. The results of these models have been summarized in Table 4. According to these findings, the LHV, HHV, and NH models perform best in the test set, with MAE, MRE, and MSE values ranging from 0.025-0.047, 1.9%-3.5%, and 0.001-0.004, respectively, followed by the H_2 model, which has MAE (0.054), MRE (3.5%), and MSE (0.001-0.004) (0.005). While the CO and CO_2 model findings are not as good as those obtained by other models, their MAE, MRE, and MSE are around 0.06, 5%, and 0.009, respectively. The highest MRE about 5% for CO_2 could be due to process parameter variation as shown in Table 1, particularly BMR, which has a more significant effect on CO and CO_2 yield than the others. Using this data, the HDMR model was developed, and the indicators MAE, MRE, and MSE were determined from it. The HHV, NHV, and NH models perform better in both training and testing. All models demonstrated remarkable generalization skills. Crossvalidations of the prediction model were performed using actual data, as shown in Figure 7. Coefficient of determinant (R^2) for the prediction of H_2 is 0.96, and the prediction values versus actual datapoints are quite close to each other in Figure 7(a). Similarly, R^2 for NH, HHV, and LHV are 0.96, 0.99, and 0.99, respectively. The prediction values and the actual datapoints are also close to each other for NH, HHV, and LHV, as presented in Figures 7(b)–7(d), respectively. Therefore, these results, R^2, MSE, MRE, and MAE, are the indicators for the better predictability of the model. Thus, the estimated values of all models correspond well with the simulated values, indicating that the predictive models of these variables are robust.

3.3. HDMR Surrogate Model Optimization. Biomass gasification model optimization has been done with the application of the HDMR-based surrogate model. Optimization has been categorized into single-objective approach and multiple-objective approach as given in Sections 3.3.1 and 3.3.2, respectively.

3.3.1. Single-Objective Optimization. HDMR-based model optimization with single objective has been done by varying the process input parameters. Mole fractions of H_2 are maximum 0.369 at 480°C temperature, 1.33 bar pressure, and 2.00 BMR but at these parameters, process is not energy-efficient due to negative NH value which reflects that external source heat is being required in the process for biomass valorization. The HHV and LHV both are maximum at 1000°C and 2.00 BMR, with 2.36 and 4.00 bar, respectively, as given in Table 5. The process is also not energy-efficient because the net heat energy is negative at these conditions. While gasification process energy efficiency in terms of net heat is remarkable at 401.7°C, 0.25 BMR, and 2.77 bar but mole fractions of H_2 are too low along with HHV and LHV values. Therefore, single-objective optimization is solely focused on one output while neglecting the other parameters given in Table 5. Hence, incorporating other variables, a multiobjective optimization could be a viable option for optimizing the gasification process which could provide an optimum solution considering HHV, LHV, mole fractions of H_2, and NH constraints.

Table 4: Model test performance summary.

Model	MAE	MRE (%)	MSE
H_2 model	0.0540	3.49	0.0048
CO model	0.0522	3.51	0.0043
CO_2 model	0.0774	5.15	0.0093
HHV model	0.0275	2.00	0.0012
LHV model	0.0254	1.90	0.0011
NH model	0.0471	3.46	0.0043

3.3.2. Multiobjective Optimization. Multiobjective optimization provides the better solution for feasible biomass gasification process. The HDMR method had been applied to obtain the multiobjective optimal solution based on the process parameters. Equation (21) is the objective function, Equation (22) is the constraints, and this model can be solved by using the KTT conditions.

$$\min - f_{M_n}(T, \text{BMR}, P), \tag{21}$$

where f_{M_n} is the HDMR surrogate model for optimization of H_2, HHV, and LHV subject to

$$\begin{aligned} \text{Temperature}(T) \text{ ranges } 400 \le T_C{}^o \le 1000 \\ \text{Pressure}(P) \text{ ranges } 1 \le P_{\text{bar}} \le 4 \\ \text{Biomass to air ration (BMR) ranges } 0.25 \le \text{BMR} \le 2 \\ f_{NH}(T, \text{BMR}, P) \ge 0 \end{aligned} \tag{22}$$

where f_{NH} is the HDMR surrogate model for predicting net heat based on T, BMR, and P.

Therefore, the HDMR model which fulfilled these model constraints has been developed. According to model results, around 765°C, 0.59 BMR, and 1 bar, the mole fraction of H_2 is 0.24, with 158.17 kJ/mol of HHV and 142.48 kJ/mol of LHV, respectively. This process is also energy-efficient because 442.37 kJ/s surplus net heat energy is being produced as per model result. Therefore, these conditions (765°C, 0.59 BMR, and 1 bar) are the optimum one which can fulfill all set constraints for the gasification process. These input parameters could be applied to get the optimum

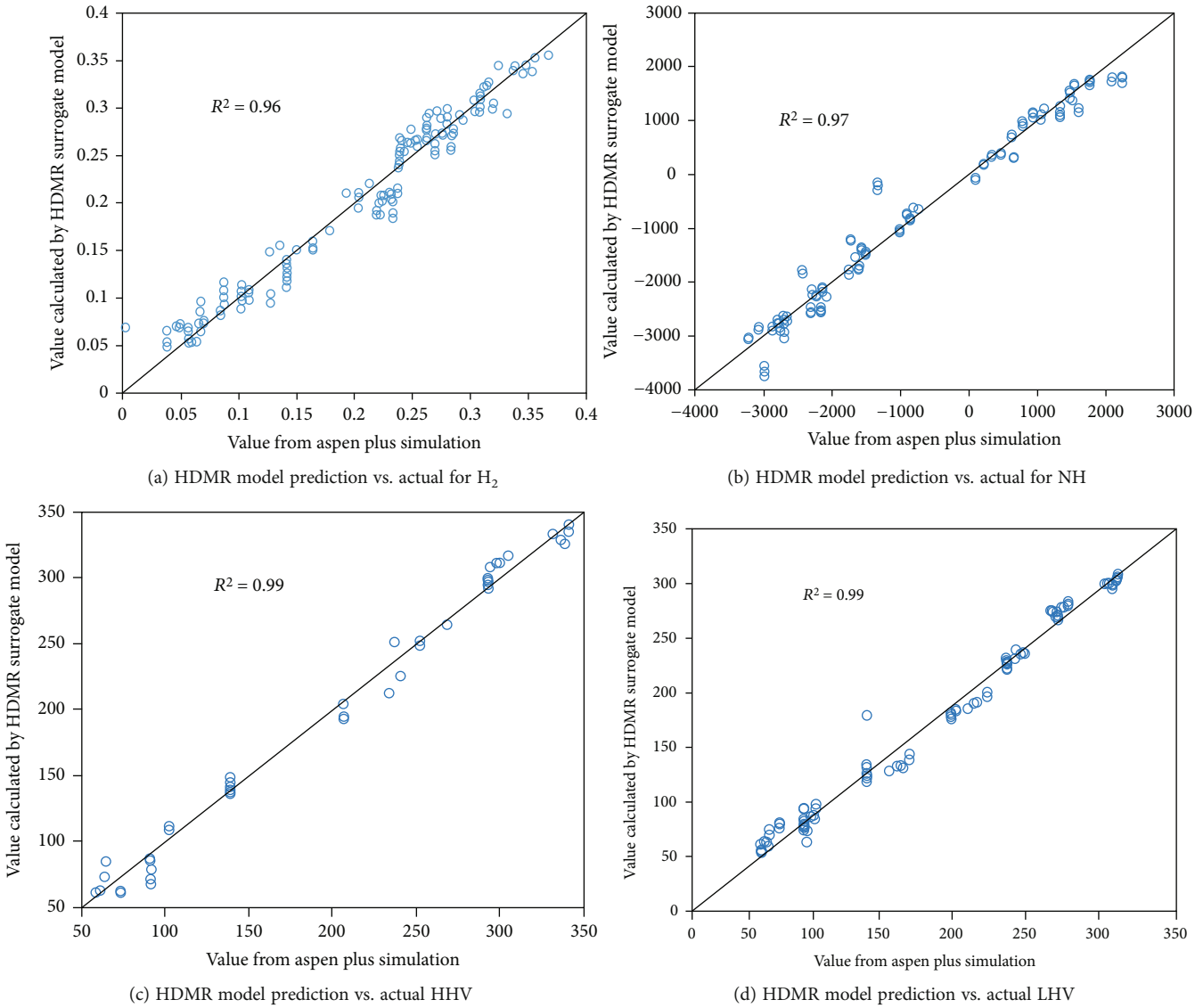

(a) HDMR model prediction vs. actual for H_2

(b) HDMR model prediction vs. actual for NH

(c) HDMR model prediction vs. actual HHV

(d) HDMR model prediction vs. actual LHV

Figure 7: HDMR model prediction values vs. actual values.

Table 5: Single-objective optimization.

Objectives	T (°C)	BMR	P (bar)	H_2 (mole frac.)	HHV (kJ/mol)	LHV (kJ/mol)	NH (kJ/s)
Max H_2	480.19	2.00	1.33	0.369	332.376	293.216	-2389.81
Max HHV	999.99	2.00	2.36	0.319	340.905	301.944	-2395.19
Max LHV	1000.00	2.00	4.00	0.320	338.757	305.400	-2348.73
Max NH	401.71	0.25	2.77	0.030	77.087	69.419	2236.67

output of gasification process in terms of better H_2, LHV, HHV, and process energy efficiency.

4. Conclusion

In this study, the HMDR-based prediction model and multi-objective optimization have been developed for biomass gasification process. The following points have been concluded based on this research:

(i) HDMR model training performances (R^2) are 0.96, 0.97, 0.99, and 0.99 for H_2, NH, HHV, and LHV, respectively, which indicate the less error in predicting output

(ii) Single-objective optimization concluded 480.19°C, 2.00 BMR, and 1.33 bar as an optimum parameter for maximum mole fractions of H_2 (0.369) but process is not energy-efficient at these parameters due to -2389.8 kJ/s of NH

(iii) Temperature and BMR are most contributing factors in the mole fractions of H_2, LHV, HHV, and NH. Multiobjective optimization results show that 765°C, 0.59 BMR, and 1 bar have the optimum output in terms of 0.24 H_2 mole fraction, 158.17 kJ/mol of HHV, 142.48 kJ/mol of LHV, and 442.37 kJ/s of NH

In the current research, HDMR could be used for biomass gasification prediction and optimization purpose because of high training performance (R^2). But this is a base model with limited input parameters and data type. For future work, the complex model which can predict and optimize the gasification process with different input parameters including multiple gasifying agents and catalyst utilization can be developed by using this technique.

Nomenclature

BM: Biomass
CGE: Cold gas efficiency
CSS: Carbon capture storage
FR: Feed rate
GHG: Greenhouse gases
HDMR: High-dimensional model representation
LHV: Lower heating value
MAE: Mean absolute error
MRE: Mean relative error
MSE: Mean square error
MC: Mix wood
NH: Net heat
PL: Poultry litter
PR: Peng Robinson Equation of State
SS: Sewage sludge saw dust
SW: Soft wood.

Data Availability

Data is available on request.

Conflicts of Interest

The authors declare that they have no conflicts of interest.

Acknowledgments

The work described in this paper was supported by a grant from the Research Grants Council of the Hong Kong Special Administrative Region, China-General Research Fund (Project ID: P0037749, Funding Body Ref. No.: 15303921, Project No.: Q88R); a grant from the Research Institute for Advanced Manufacturing (RIAM), the Hong Kong Polytechnic University (PolyU) (Project No.: 1-CD4J, Project ID: P0041367); a grant from Research Centre for Resources Engineering towards Carbon Neutrality (RCRE), the Hong Kong Polytechnic University (PolyU) (Project No.: 1-BBEC, Project ID: P0043023); and the Research Committee of the Hong Kong Polytechnic University under student account code RHWR..

Supplementary Materials

Detail of HDMR model coefficients is given in supplementary information for H_2 (Table S1), CO (Table S2), CO_2 (Table S3), HHV (Table S4), LHV (Table S5), and NH (Table S6), respectively. *(Supplementary Materials)*

References

[1] Z. Abdin, A. Zafaranloo, A. Rafiee, W. Mérida, W. Lipiński, and K. R. Khalilpour, "Hydrogen as an energy vector," *Renewable and Sustainable Energy Reviews*, vol. 120, article 109620, 2020.

[2] Y. Ayub, A. Mehmood, J. Ren, and C. K. M. Lee, "Sustainable recycling of poultry litter to value-added products in developing countries of South Asia," *Journal of Cleaner Production*, vol. 357, article 132029, 2022.

[3] Y. Fang, M. C. Paul, S. Varjani, X. Li, Y.-K. Park, and S. You, "Concentrated solar thermochemical gasification of biomass: principles, applications, and development," *Renewable and Sustainable Energy Reviews*, vol. 150, article 111484, 2021.

[4] S. Verma, A. M. Dregulo, V. Kumar et al., "Reaction engineering during biomass gasification and conversion to energy," *Energy*, vol. 266, article 126458, 2023.

[5] N. Mazaheri, A. H. Akbarzadeh, E. Madadian, and M. Lefsrud, "Systematic review of research guidelines for numerical simulation of biomass gasification for bioenergy production," *Energy Conversion and Management*, vol. 183, pp. 671–688, 2019.

[6] Y. Ayub, S. Tao, J. Ren, C. K. M. Lee, C. He, and A. Manzardo, "Poultry litter valorization by application of hydrothermal gasification: process simulation, economic, energic, and environmental analysis," *International Journal of Energy Research*, vol. 46, no. 15, pp. 23095–23109, 2022.

[7] S. Singh Siwal, Q. Zhang, C. Sun, S. Thakur, V. Kumar Gupta, and V. Kumar Thakur, "Energy production from steam gasification processes and parameters that contemplate in biomass gasifier - a review," *Bioresource Technology*, vol. 297, article 122481, 2020.

[8] T. Srinivas, A. V. S. S. K. S. Gupta, and B. V. Reddy, "Thermodynamic equilibrium model and exergy analysis of a biomass gasifier," *Journal of Energy Resources Technology*, vol. 131, no. 3, 2009.

[9] P. Baggio, M. Baratieri, L. Fiori, M. Grigiante, D. Avi, and P. Tosi, "Experimental and modeling analysis of a batch gasification/pyrolysis reactor," *Energy Conversion and Management*, vol. 50, no. 6, pp. 1426–1435, 2009.

[10] R. Knappstein, G. Kuenne, H. Nicolai, F. di Mare, A. Sadiki, and J. Janicka, "Description of the char conversion process in coal combustion based on premixed FGM chemistry," *Fuel*, vol. 236, pp. 124–134, 2019.

[11] K. I. M. Al-Malah, *Aspen Plus Chemical Engineering Applications*, John Wiley & Sons, Inc., New Jersey, 2017.

[12] M. Vascellari, R. Arora, and C. Hasse, "Simulation of entrained flow gasification with advanced coal conversion submodels. Part 2: char conversion," *Fuel*, vol. 118, pp. 369–384, 2014.

[13] Q. Dang, X. Zhang, Y. Zhou, and X. Jia, "Prediction and optimization of syngas production from a kinetic-based biomass gasification process model," *Fuel Processing Technology*, vol. 212, article 106604, 2021.

[14] N. Hashimoto, R. Kurose, S.-M. Hwang, H. Tsuji, and H. Shirai, "A numerical simulation of pulverized coal combustion employing a tabulated- devolatilization-process model (TDP model)," *Combustion and Flame*, vol. 159, no. 1, pp. 353–366, 2012.

[15] J. Xing, K. Luo, H. Pitsch et al., "Predicting kinetic parameters for coal devolatilization by means of artificial neural networks," *Proceedings of the Combustion Institute*, vol. 37, no. 3, pp. 2943–2950, 2019.

[16] H. O. Kargbo, J. Zhang, and A. N. Phan, "Optimisation of two-stage biomass gasification for hydrogen production via artificial neural network," *Applied Energy*, vol. 302, article 117567, 2021.

[17] S. Ascher, W. Sloan, I. Watson, and S. You, "A comprehensive artificial neural network model for gasification process prediction," *Applied Energy*, vol. 320, article 119289, 2022.

[18] M. Pan, J. Sikorski, J. Akroyd, S. Mosbach, R. Lau, and M. Kraft, "Design technologies for eco-industrial parks: from unit operations to processes, plants and industrial networks," *Applied Energy*, vol. 175, pp. 305–323, 2016.

[19] H. Rabitz and Ö. F. Aliş, "General foundations of high-dimensional model representations," *Journal of Mathematical Chemistry*, vol. 25, no. 2, pp. 197–233, 1999.

[20] G. Brownbridge, P. Azadi, A. Smallbone, A. Bhave, B. Taylor, and M. Kraft, "The future viability of algae-derived biodiesel under economic and technical uncertainties," *Bioresource Technology*, vol. 151, pp. 166–173, 2014.

[21] P. Azadi, G. Brownbridge, S. Mosbach, O. Inderwildi, and M. Kraft, "Simulation and life cycle assessment of algae gasification process in dual fluidized bed gasifiers," *Green Chemistry*, vol. 17, no. 3, pp. 1793–1801, 2015.

[22] D. K. Singh and J. V. Tirkey, "Modeling and multi-objective optimization of variable air gasification performance parameters using Syzygium cumini biomass by integrating ASPEN Plus with response surface methodology (RSM)," *International Journal of Hydrogen Energy*, vol. 46, no. 36, pp. 18816–18831, 2021.

[23] Q. Xie, H. Liu, D. Bo, C. He, and M. Pan, "Data-driven modeling and optimization of complex chemical processes using a novel hdmr methodology," in *Computer Aided Chemical Engineering*, M. R. Eden, M. G. Ierapetritou, and G. P. Towler, Eds., vol. 44, pp. 835–840, Elsevier, 2018.

[24] W. Han, Z. Sun, A. Scholtissek, and C. Hasse, "Machine learning of ignition delay times under dual-fuel engine conditions," *Fuel*, vol. 288, article 119650, 2021.

[25] L. T. Biegler, Y.-D. Lang, and W. Lin, "Multi-scale optimization for process systems engineering," *Computers & Chemical Engineering*, vol. 60, pp. 17–30, 2014.

[26] J. Favas, E. Monteiro, and A. Rouboa, "Hydrogen production using plasma gasification with steam injection," *International Journal of Hydrogen Energy*, vol. 42, no. 16, pp. 10997–11005, 2017.

[27] F. Kartal and U. Özveren, "A deep learning approach for prediction of syngas lower heating value from CFB gasifier in Aspen plus®," *Energy*, vol. 209, article 118457, 2020.

[28] N. Striūgas, K. Zakarauskas, A. Džiugys, R. Navakas, and R. Paulauskas, "An evaluation of performance of automatically operated multi-fuel downdraft gasifier for energy production," *Applied Thermal Engineering*, vol. 73, no. 1, pp. 1151–1159, 2014.

[29] A. Gagliano, F. Nocera, M. Bruno, and G. Cardillo, "Development of an equilibrium-based model of gasification of biomass by Aspen Plus," *Energy Procedia*, vol. 111, pp. 1010–1019, 2017.

[30] D. K. Singh and J. V. Tirkey, "Process modelling and thermodynamic performance optimization of biomass air gasification fuelled with waste poultry litter pellet by integrating Aspen plus with RSM," *Biomass and Bioenergy*, vol. 158, article 106370, 2022.

[31] M. Puig-Gamero, D. T. Pio, L. A. C. Tarelho, P. Sánchez, and L. Sanchez-Silva, "Simulation of biomass gasification in bubbling fluidized bed reactor using Aspen Plus®," *Energy Conversion and Management*, vol. 235, article 113981, 2021.

[32] T. Chai and R. R. Draxler, "Root mean square error (RMSE) or mean absolute error (MAE)? – arguments against avoiding RMSE in the literature," *Geoscientific Model Development*, vol. 7, no. 3, pp. 1247–1250, 2014.

[33] G. Li and H. Rabitz, "Ratio control variate method for efficiently determining high-dimensional model representations," *Journal of Computational Chemistry*, vol. 27, no. 10, pp. 1112–1118, 2006.

[34] W. Wang and Y. Lu, "Analysis of the mean absolute error (MAE) and the root mean square error (RMSE) in assessing rounding model," *IOP Conference Series: Materials Science and Engineering*, vol. 324, article 012049, 2018.

[35] A. Di Bucchianico, "Coefficient of determination (R^2)," in *Encyclopedia of Statistics in Quality and Reliability*, Wiley, 2008.

[36] R. H. Byrd, J. C. Gilbert, and J. Nocedal, "A trust region method based on interior point techniques for nonlinear programming," *Mathematical Programming*, vol. 89, no. 1, pp. 149–185, 2000.

[37] R. A. Waltz, J. L. Morales, J. Nocedal, and D. Orban, "An interior algorithm for nonlinear optimization that combines line search and trust region steps," *Mathematical Programming*, vol. 107, no. 3, pp. 391–408, 2006.

[38] L. T. Biegler, A. M. Cervantes, and A. Wächter, "Advances in simultaneous strategies for dynamic process optimization," *Chemical Engineering Science*, vol. 57, no. 4, pp. 575–593, 2002.

[39] T. Detchusananard, K. Im-orb, P. Ponpesh, and A. Arpornwichanop, "Biomass gasification integrated with CO2 capture processes for high-purity hydrogen production: process performance and energy analysis," *Energy Conversion and Management*, vol. 171, pp. 1560–1572, 2018.

[40] Y. Ayub, J. Ren, T. Shi, W. Shen, and C. He, "Poultry litter valorization: development and optimization of an electrochemical and thermal tri-generation process using an extreme gradient boosting algorithm," *Energy*, vol. 263, article 125839, 2023.